SELF-DIFFUSION IN ISOTROPIC DISPERSIONS OF COLLOIDAL RODS

M. P. B. VAN BRUGGEN*, J. K. G. DHONT AND H. N. W. LEKKERKERKER.
Van 't Hoff laboratory for Physical- and Colloid Chemistry, Debye Institute, Utrecht University, Padualaan 8, 3584 CH Utrecht, The Netherlands.

The long-time self-diffusion coefficient DsL of charge stabilized colloidal rods was measured as a function of concentration in the isotropic phase by means of fluorescence recovery after photobleaching. A linear decrease of DsL is found to concentrations well within the semi-dilute regime. When the diameter of the rods is large compared to the Debye length, the concentration dependence is in agreement with Brownian dynamics (BD) simulations on hard spherocylinders, using an effective diameter for the rods. However in case of thin rods, a much stronger decrease of DsL is found experimentally than is predicted by the BD simulations with an effective diameter.

1. Introduction

Solutions containing rodlike polymers, macromolecules or colloids are called "dilute" at volume fractions below $(D/L)^2$, with D the diameter and L the length of the rods[1]. For volume fractions larger than $(D/L)^2$ the volume swept out by the thermally rotating rods equals the system size so that rotational diffusion will be become significantly hindered. The solution is called "semi-dilute". At volume fractions larger than (D/L), the total excluded volume of the rods equals the system size and translational diffusion will become significantly hindered as well, the solution is now called "concentrated". Upon further concentration, above a certain threshold concentration the solution may spontaneously phase separate into an orientationally ordered, liquid crystalline phase and a disordered isotropic phase. *Large* differences in both dynamics and phase behavior can thus evolve at *low* volume fractions when rods are long and thin. In this paper we will focus on diffusion of rods in isotropic solutions.

Diffusion of rodlike particles has been studied theoretically[2-7] as well as with computer simulation[8-14]. Experimentally, dynamic light scattering has proven to be a powerful tool in measuring translational and rotational diffusion of rodlike particles

in dilute solutions[15-19]. Techniques like forced Rayleigh scattering (FRS) and fluorescence recovery after photobleaching (FRAP) monitor translational diffusion of individual particles and can be applied over the whole concentration range. The few FRAP- and FRS-studies reported in literature deal with semi-flexible macromole-cules such as DNA[20,21], poly(γ-benzyl α,L-glutamate) (PBLG)[22] and polymerising F-actin[23]. Since flexibility alters translational diffusion[1], we recently performed FRAP measurements on fluorescent, *rigid* colloidal silica rods[24]. In the present paper these results are combined with additional FRAP measurements on dispersions of fluorescent, rigid colloidal boehmite rods. An extensive report of FRAP measurements on rigid rods, including TMV and fd viruses, in the isotropic as well as in the *nematic* phase is in preparation[25].

2. Synthesis and Characterisation

2.1. Fluorescent Boehmite Rods

Boehmite (γ-AlOOH) needles were synthesised according to a procedure developed by Buining *et al.*[26]. The aluminum precursors in this synthesis are the aluminum alkoxides aluminum-iso-propoxide (AIP 98%, Janssen chemica) and aluminum sec-butoxide (ASB, Fluka chemica). The precursors were dissolved in water which had been acidified with hydrochloric acid (37%, Merck). After one week of mixing, the mixture was brought under hydrothermal conditions (150°C, 4 atm.) in an autoclave. Finally the dispersion was dialysed thoroughly against flowing demineralised water. More details about the synthesis can be found in ref. 26.

Boehmite rods were stabilised with aluminum chlorohydrate ($Al_2(OH)_5Cl$ 2-$3H_2O$,"Locron p", Hoechst) by adding 0.5 g of aluminum chlorohydrate, further abreviated to ACH to 100 g of a 8g/l boehmite dispersion. These rods were labelled with FITC (FITC isomer I, Sigma) and the remaining free dye was removed by centrifugation, leaving a yellowish coloured supernatant and a deep yellow, transparent sediment. The sediment was easily redispersed with a 0.01 M NaCl (p.a.) solution. The dispersion code used hereafter is BACH. More details about the synthesis and properties of ACH stabilised boehmite rods will be given in a forthcoming paper[27].

2.2. *Fluorescent Silica Rods*

Boehmite rods were coated with silica by a recently developed coating procedure[28]. First the rods are grown in a sodium silicate ($Na_2Si_3O_7$, Fluka) solution, followed by growth in a two-phase system of tetraethoxysilane (TES, Fluka) and an ammonia (25%, Merck)-water mixture. In the third step the rods are transferred to a mixture of ethanol, water, ammonia and tetra ethoxysilane, often referred to as a Stöber mixture[29], and the rods can be grown to any desired aspect ratio. These "silica rods" were labelled with FITC according to the method of Van Blaaderen *et al.*[30]. Finally the solvent was changed from water-ethanol to DMF and the salt concentration was adjusted to 0.01 M with lithium chloride (p.a.). These fluorescent, silica coated boehmite rods are hereafter referred to as BS.

2.3. *Transmission Electron Microscopy*

Transmission electron microscopy (TEM) was performed on a Philips CM10 microscope. Samples were prepared by dipping formvar coated, copper grids into a very dilute aqueous dispersion to which 50% ethanol was added to promote spreading of the solvent on the hydrophobic formvar. Micrographs of the BACH and BS rods are given in figures 2.1a and 2.1b.

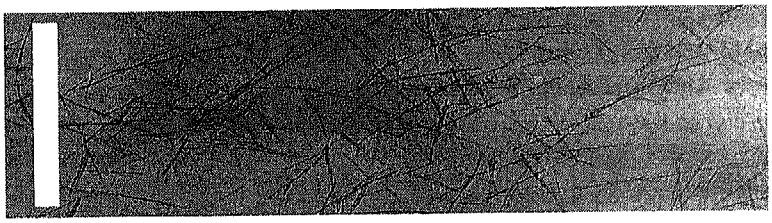

Figure 2.1a. TEM micrograph of boehmite rods stabilised with ACH. Bar represents 1μm.

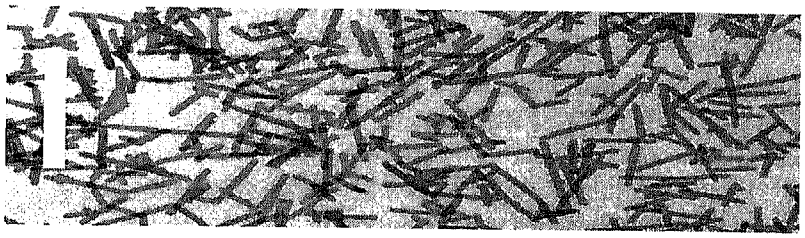

Figure 2.1b. TEM micrograph of silica rods. Bar represents 1μm.

Dimensions and standard deviation (σ) of the rods were obtained using an interactive image analysis program and the results are summarised in table 2.1.

Table 2.1. Average rod dimensions and standard deviations

System	<L> (nm)	σ_L (nm)	<D> (nm)	σ_D (nm)	L/D
BACH	257	72	9.4	1.8	19*
BS	323	133	46	5	7

*Aspect ratio corrected for the presence of aluminum chlorohydrate;

2.4. Stability and Phase Behaviour

Both the BACH and BS dispersions are stable in 0.01 M LiCl and NaCl over periods of months. Upon concentration, the systems spontaneously phase separate into a nematic and an isotropic phase. For the BACH system macroscopic phase separation occurred within 1 to 2 weeks at volume fractions higher than 1.9 %. In the BS dispersion the onset of phase separation was observed in the sediment of a settling dispersion[24] when the concentration of the sediment had reached approximately 26%. In both systems phase separation proceeds by the formation of spindle shaped nematic droplets (tactoids) which are clearly visible under the polarisation microscope due to the intrinsic birefringence of the crystalline boehmite rods.

Table 2.2. Dispersion properties

System	solvent	n_s	κ^{-1} (nm)	ϕ_I (%)	ϕ_N (%)
BACH	water	1.33	3.0	1.9	3.3**
BS	DMF	1.43	2.2	26	--

n_s is the refractive index of the solvent and κ^{-1} is the Debye length. **Estimated by extrapolating the relative amount of nematic phase v.s. the volume fraction to unity.

The dispersion properties are summarised in table 2.2. The volume fraction at which the isotropic phase becomes unstable with respect to the nematic phase is denoted as ϕ_I, for the nematic phase this is ϕ_N.

2.5. Dynamic Light Scattering

The diffusion coefficient at infinite dilution D_0 was measured with dynamic light scattering (DLS) in very dilute samples so that concentration effects on the diffusion coefficient are negligible small. An krypton laser (Spectra Physics 2020, λ=647.1 nm) was used to minimise heating effects due to absorption of light by FITC. Scattering angles θ ranged from 30° to 120°. The intensity auto correlation functions (IACF's) were fitted to single exponentials, including a second cumulant to account for polydispersity: $\alpha + \beta\exp(-b(K)t + c(K)t^2)$, with b(K) the decay exponent, c(K) the second cumulant and K the wave vector which is given by:

$$K = \frac{4\pi n_m}{\lambda} \sin\frac{\theta}{2}, \tag{2.1}$$

where λ is the wavelength of the light in vacuo and n_m the refractive index of the medium. For K<5/L, the contribution of rotational diffusion to the decay of the IACF is relatively small and b(K) is equal to $2D_0K^2$. The measured diffusion coefficients are compared with the theoretical diffusion coefficient at infinite dilution[31],

$$D_0 = \frac{k_B T}{3\pi\eta_m L}\left[ln\left(\frac{L}{D}\right) + 0.316 + 0.5825\frac{D}{L} + 0.050\left(\frac{D}{L}\right)^2\right], \phi \to 0, \tag{2.2}$$

with k_B the Boltzmann constant and T the absolute temperature. The results are summarised in table 2.3.

Table 2.3. D_0 measured with DLS compared to the theoretical value.

System	D_0^{DLS} (10^{-13} m^2s^{-1})	$D_0^{th.}$ (10^{-13} m^2s^{-1})
BACH	30	55
BS	18	36

It appears that the theoretical value of the diffusion coefficient is always higher than the experimental value. Surface irregularities leading to a higher friction factor as well as polydispersity may explain this discrepancy.

3. Self-diffusion Measurements with FRAP

In the present FRAP set-up a sinusoidal fringe pattern is produced by two interfering laser beams which intersect in the dispersion[32-35]. The fringe pattern is bleached in the dispersion at high laser intensity and the *decay* of the fringe amplitude due to diffusion of the rods is monitored at reduced laser intensity. The decay of the FRAP signal is equivalent to the *recovery* of the fluorescence in the regions where the bleach intensity was large. Technical details about the FRAP set-up as used in this study can be found in ref's 32-35. The wave vector associated with the fringe pattern is equal to:

$$K = \frac{4\pi}{\lambda} sin\left(\frac{\theta}{2}\right), \tag{3.1}$$

with θ the intersection angle of the two incident laser beams and λ the wavelength in vacuo. Note that the wave vector K in a FRAP experiment does not contain the refractive index of the solvent. The wavelength of the sinusoidal bleach pattern, which will be referred to as the fringe spacing, is equal to $2\pi/K$ and can be varied via θ. One can derive that the decay of the fringe amplitude S(t) is given by:

$$S(t) \propto exp(-K^2 D_s^L t), \tag{3.2}$$

with D_s^L the long-time self-diffusion coefficient[34]. At sufficiently small values of θ, and consequently for fringe spacings much larger than the particle's size, $d\ln S(t)/d(K^2 t)$ indeed remained constant and its value is equal to D_s^L.

Samples were transferred into long thin glass cuvettes (Vitrodynamics inc.) with a pathlength of 100 μm and a width of 1 mm or 2 mm. The blue line (488 nm) of an argon ion laser (Spectra Physics 2000) was used. At this wavelength fluorescence of FITC is maximal. Long-time self diffusion coefficients were obtained by fitting the decay curve to the single exponential as given by Eq.(3.2). In contrast to DLS, no second cumulant had to be taken into account for obtaining good fits. The results of measurements in the isotropic phase are given in figure 3.1. Initially a linear dependency between D_s^L/D_0 and the volume fraction is found. D_0 was obtained by linear extrapolation to ϕ=0. In the BACH dispersion this linear dependency starts to deviate at ϕ = 0.0063, in the BS dispersion this is at approximately ϕ = 0.15. These volume fractions correspond to $(L/D)^2\phi$ of 2 and 7 respectively.

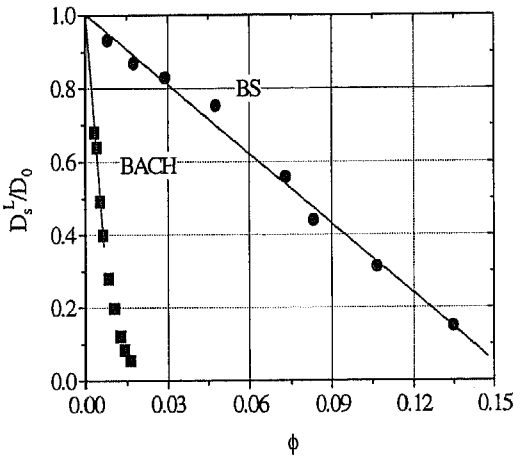

Figure 3.1. Concentration dependence of the long-time self diffusion coefficient of boehmite rods (■) and silica rods[24] (●).

Apparently up to concentrations in the semi-dilute regime, D_s^L can be written as:

$$D_s^L = D_0 \ (1 - \alpha\phi) \tag{3.3}$$

with α the slope of D_s^L/D_0 versus the volume fraction and D_0 the diffusion coefficient at infinite dilution. The results are summarised in table 3.1.

Table 3.1. FRAP-data

System	$D_0^{FRAP}(10^{-13}\ m^2s^{-1})$	$-\alpha$	$-\alpha_{eff}$	$(L/D)_{eff}$
BACH	30.0	94.9± 9.8	12.1± 1.3	6.8
BS	19.0	6.3 ± 0.3	3.71± 0.2	5.4

The FRAP value of D_0 is consistent with the value obtained with DLS. The subindex "eff" used in table 3.1 will be explained in the next paragraph.

4. Discussion

Our data are rather similar with the experimental data found for *hard*, spherical particles for which also a linear decrease of D_s^L is observed over a wide range of concentrations[33,34]. Moreover, the experimental slope of D_s^L/D_0 versus ϕ for spherical particles is in accordance with the theoretically predicted (including hydrodynamics) first order coefficient of Batchelor[36] and Cichocki and Felderhof[37]. For rodlike particles such an expression is still lacking. Any of the self-diffusion measurements on semi-flexible macromolecules[20-23] show this feature. Deviation from linearity is observed in the semi-dilute concentration regime, at rescaled volume fractions ϕ/ϕ_I equal to 0.6 for the BS dispersion, and 0.3 for the BACH dispersion.

Löwen[38] recently performed Brownian Dynamics (BD) simulations on *hard* spherocylinders with aspect ratios up to 6. In this simulation only excluded volume interactions are considered, hydrodynamic interactions are neglected. Löwen gives an expression for the first order in ϕ coefficient obtained by fitting the simulation data to a function in powers of the aspect ratio.

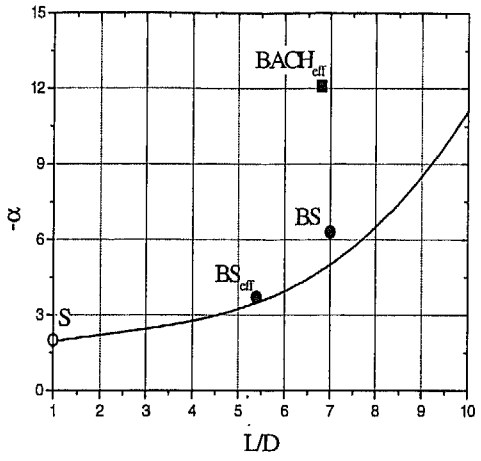

Figure 4.1. The slope α of D_s^L/D_0 versus the aspect ratio for hard silica spheres[34] (O), boehmite rods (■) and silica rods (●). The sub-index "eff" implies that volume fraction and aspect ratio are corrected for double layer repulsion. The solid line represents the BD simulation result[38].

In order to compare our data with the BD simulation, the dimensions of the rods are mapped on an effective hard-core potential by assuming that rods can approach each other until their double layer repulsion has become 1 k_BT[24]. Consequently the volume fraction transforms in to an "effective" volume fraction ϕ_{eff} and the aspect ratio in to an "effective" aspect ratio $(L/D)_{eff}$. The slope after correcting for this effect are also given in table 3.1 and is denoted as α_{eff}. The value of the slope before and after correction together with the fit function of Löwen are shown in figure 4.1. For completeness the experimental data on hard spherical particles of Imhof *et al.*[34] are given too. The uncorrected slope of the BACH dispersion is omitted in figure 4.1 because Löwen's prediction is thought to be valid for L/D < 10. Mapping the dimensions of the BS rods on an effective hard-core potential yields good agreement with the BD results. However for the BACH rods potential-mapping clearly fails. Here we measure a much *stronger* concentration dependency. Likely mapping the real potential onto a hard-core potential is only legitimate when $\kappa^{-1} \ll D$. For the BS rods $\kappa D=21$, for the BACH system this is only 4. In addition it is unclear how important hydrodynamic interactions are.

5. Conclusions

In this paper long-time self-diffusion measurements on two new model systems of fluorescent, rigid colloidal rods were performed using fluorescence recovery after photobleaching (FRAP). The measurements show an initial linear dependency of the long-time self-diffusion coefficient with concentration, which becomes non-linear at higher concentration. A linear dependency over a wide range of concentrations is also found for hard spherical particles[34,35]. The experimental slopes of D_s^L/D_0 versus the volume fraction were compared with BD simulations of hard-spherocylinders[38], by mapping the rod dimensions on an effective hard-core potential. For silica rods with diameters much larger than the Debye length, this procedure yields good agreement with the BD simulations. For much thinner boehmite rods agreement is not satisfactory.

Acknowledgements
Hoechst AG Augsburg (Gemany) kindly provided the aluminum chlorohydrate. This work was supported by The Netherlands Foundation for Chemical research (SON) with financial aid from the Netherlands Organisation for Scientific Research (NWO).

References

1. Doi M. and Edwards S. F., *The Theory of Polymer Dynamics*, (Clarendon Press, Oxford, 1986), 324.
2. Doi M. and Edwards S. F., *J. Chem. Soc. Faraday Trans. 2* **74** (1978), 560.
3. Edwards S. F. and Evans K. E., *J. Chem. Soc. Faraday Trans. 2* **78** (1982), 113.
4. Sato T. and Teramoto A., *Macromolecules* **24** (1991), 193.
5. Teraoka I. and Hayakawa R., *J. Chem. Phys.* **89** (1988), 6989.
6. Szamel G., *Phys. Rev. Lett.* **70** (1993), 3744.
7. Odijk T., *Macromolcules* **19** (1986), 2073.
8. Frenkel D. and Maguire J. F., *Mol. Phys.* **49** (1983), 503.
9. Magda J. J., Davis H. T. and Tirrell M., *J. Chem. Phys.* **85** (1986), 6674.
10. Doi M., Yamamoto I. and Kano F., *J. Phys. Soc. Jap.* **53** (1984), 3000.
11. Bitsanis I., Davis H. T. and Tirrell M., *Macromolecules* **21** (1988), 2824.
12. Bitsanis I., Davis H. T. and Tirrell M., *Macromolecules* **23** (1990), 1157.
13. Branka A. C. and Heyes D. M., *Phys. Rev. E* **50** (1994), 4810.
14. Kirchhoff Th., Löwen H. and Klein R., *Phys. Rev. E* **53** (1996), 5011.
15. Kam Z., Borochov N. and Eisenberg H., *Biopolymers* **20** (1981), 2671.
16. Zero K. M. and Pecora R., *Macromolecules* **15** (1982), 87.
17. Kubota K., Urabe H., Tominaga Y. and Fujime S., *Macromolecules* **17** (1984), 2096.
18. Fujime S., Takasaki-Ohsita M. and Maeda T., *Macromolecules* **20** (1987), 1292 .
19. DeLong L. M. and Russo P. S., *Macromolecules* **24** (1991), 6139.
20. Wang L., Garner M. M. and Yu H., *Macromolecules* **24** (1991), 2368.
21. Scalettar B. A., Hearst J. E. and Klein M. P., *Macromolecules* **22** (1989), 4550.
22. Bu Z., Russo P. S., Tipton D. L. and Negulescu I. I., *Macromolecules* **27** (1994), 6871.
23. Tait J. F. and Frieden C., *Biochemistry* **21** (1982), 3666.
24. van Bruggen M. P. B., Lekkerkerker H. N. W. and Dhont J. K. G., *Phys. Rev. E* **56**, 4394 (1997).
25. van Bruggen M. P. B., Peetermans J., Federle G., Lekkerkerker H. N. W., Maret G. and Dhont J. K. G., in preparation.
26. Buining P. A., Pathmamanoharan C., Jansen J. B. H. and Lekkerkerker H. N. W., *J. Am. Ceram. Soc.* **74** (1991),1303.

27. van Bruggen M. P. B., Donker M., Lekkerkerker H. N. W. and Hughes T. L., in preparation.
28. van Bruggen M. P. B., submitted for publication.
29. Stöber W., Fink A. and Bohn E., *J. Colloid Interface Sci.* **26** (1968), 62.
30. van Blaaderen A. and Vrij A., *Langmuir* **8** (1992), 2921.
31. Tirado M. M., Martinez C. L. and de la Torre J. G., *J. Chem. Phys.* **81** (1984), 2047.
32. Lanni F. and Ware B. R., *Rev. Sci. Instrum.* **53** (1982), 905.
33. Davoust J., Devaux P. F. and Leger L., *EMBO J.* **1** (1982), 1233.
34. Imhof A., van Blaaderen A., Maret G., Mellema J. and Dhont J. K. G., *J. Chem. Phys.* **100** (1994), 2170.
35. van Blaaderen A., Peetermans J., Maret G. and Dhont J. K. G., *J. Chem. Phys.* **96** (1992), 4591.
36. Batchelor G. K., *J. Fluid Mech.* **131** (1983), 155.
37. Cichocki B. and Felderhof B. U., *J. Chem. Phys.* **89** (1988), 3705 .
38. Löwen H., *Phys. Rev. E* **50** (1994), 1232.